Nonlinear features of two-plasmon decay in a long-scale-length plasma

D. R. Dimitrijević* and M. S. Jovanović
Department of Physics, Faculty of Sciences and Mathematics, University of Niš, P. O. Box 224, 18001 Niš, Yugoslavia
(Received 9 July 2002; published 19 November 2002)

A transparent model of two-plasmon decay in a spatially homogeneous or long-scale-length plasma, reproducing the main experimentally observed nonlinear features, is presented. Secondary coupling between the plasma waves and the ion-acoustic waves, including their frequency mismatch, proves to be the principal saturation mechanism of the instability. The wave amplitude time evolution and spectra as well as the hot-electron generation properties are compared to the experimental data.

DOI: 10.1103/PhysRevE.66.056408 PACS number(s): 52.35.Mw, 52.38.Dx

I. INTRODUCTION

Two-plasmon decay (TPD) is a nonlinear parametric instability of a large amplitude electromagnetic wave, which decays into two electron plasma waves at the quarter-critical density [1,2]. The main cause of the sustained interest in this instability, especially relative to laser-plasma fusion applications, is its potential for generating suprathermal (hot) electrons, capable of preheating the laser fusion pellet [3,4]. These hot electrons are accelerated through the mechanism of electron trapping by the plasma waves to energies determined by the phase velocity of the plasmon ($T_h \sim m v_{ph}^2/2$). Since it can be of the order of the speed of light, the detrimental effect of the instability can become quite considerable. The initial, linear phase of this instability has been studied in detail during recent decades, providing us with fairly correct concepts of the linear growth rate and homogeneous and inhomogeneous instability thresholds, as well as its interplay with other parametric instabilities [5–10]. There are, however, numerous questions concerning the nonlinear nature of TPD that need further study.

The aim of this paper is to offer a transparent model of TPD in a spatially homogeneous or long-scale-length plasma that includes a number of its most prominent nonlinear features: pump depletion, nonlinear coupling with ion modes including the frequency mismatch between secondarily induced waves, hot-electron generation, and both collisional and noncollisional sink terms in the equations for plasma waves and hot electrons, providing saturation in a stationary or quasiperiodic regime.

The paper is organized as follows. In Sec. II, the physical model is introduced that describes the temporal evolution of the slowly varying amplitudes of the waves taking part in the process, supplemented by the equations for hot-electron generation. The model equations are simulated using the appropriate numerical scheme and the corresponding results are presented and discussed in Sec. III. Finally, brief conclusions of the present work are given in the Summary section.

II. PHYSICAL MODEL

We consider propagation of a linearly polarized high-intensity laser radiation in a preformed long-scale-length plasma, i.e., an inhomogeneous plasma with characteristic density scales L of hundreds to thousands of vacuum laser wavelengths. In such plasmas a number of parametric decay instabilities occur, particularly if the laser intensities are well above the linear instability thresholds for these processes [1,2]. We address our interest here to two-plasmon decay, which implies a nonlinear coupling of a transverse pump wave to two electron plasma waves (plasmons), whose frequencies and wave vectors satisfy the well-known matching conditions $(\omega_0,\mathbf{k}_0)=(\omega_1,\mathbf{k}_1)+(\omega_2,\mathbf{k}_2)$. Since the daughter-wave frequencies ω_1 and ω_2 are near the electron plasma frequency ω_p, the occurrence of the TPD instability is clearly localized to a region near the quarter-critical density, namely, at somewhat lower densities if the electron plasma temperature is taken into account. An important item in plasma instability studies is the mechanisms leading to growth saturation. Many experimental and simulation studies [5,8,11–14] have indicated an efficient coupling of the plasma wave electrostatic energy to shorter-wavelength ion density fluctuations $(\omega_s,\mathbf{k}_s)$. We will assume that the most efficient is a secondary process in which the induced ion wave couples to the two daughter plasma waves [8,13], so that the matching conditions $(\omega_s,\mathbf{k}_s)=(\omega_1,\mathbf{k}_1)-(\omega_2,\mathbf{k}_2)$ are satisfied to the best possible extent. It is clear that this secondary coupling is not perfect and the corresponding frequency mismatch $\Delta\omega=\omega_2+\omega_s-\omega_1$ should be taken into account when writing down the equations of the system evolution. Thus, the starting equations for the slowly varying amplitudes of the coupled waves, from the fluid and Maxwell equations, read

$$
\begin{aligned}
&(\partial_t+\mathbf{v}_0\cdot\boldsymbol{\nabla})E_0=-A\,\delta n_1\delta n_2,\\
&(\partial_t+\mathbf{v}_1\cdot\boldsymbol{\nabla}+\nu_1)\,\delta n_1=AE_0\,\delta n_2^*+A_1\,\delta n_2\delta n_s,\\
&(\partial_t+\mathbf{v}_2\cdot\boldsymbol{\nabla}+\nu_2)\,\delta n_2=AE_0\,\delta n_1^*-A_1\,\delta n_1\delta n_s^*,\\
&(\partial_t+\mathbf{c}_s\cdot\boldsymbol{\nabla}+\nu_2)\,\delta n_s=-A_2E_0\,\delta n_1\delta n_2^*,
\end{aligned}
\tag{1}
$$

where $\mathbf{v}_{0,1,2}$ are the group velocities of the pump wave and daughter plasma waves, respectively, $\mathbf{c}_s$ is the ion sound speed, E_0 is the pump wave amplitude, $\delta n_{1,2}$ is the density fluctuation amplitudes assigned to the plasma waves, and $\nu_{1,2}$ are their damping rates combined from the collisional and Landau damping rates, including the influence of the hot-

*Email address: dimke@junis.ni.ac.yu

electron population on the electron plasma wave (EPW) Landau damping [15]. The coupling coefficients are given by the expressions $A=ek_\perp(k_1^2-k_2^2)/4m\omega_p k_1 k_2$, $A_1=e\omega_p|\mathbf{k}_1\cdot\mathbf{k}_2|/2mv_e^2 k_1 k_2 k_s$, and $A_2=ek_s^2 c_s|\mathbf{k}_1\cdot\mathbf{k}_2|/2m\omega_p^2 k_1 k_2$, where ω_p is the electron plasma frequency.

Next, we derive the equations for the hot-electron generation rate, assuming that the temporal gain of hot-electron energy density equals the energy taken away from the plasma waves by their collisionless damping:

$$dW_h/dt=\nu_L W_{EPW}, \tag{2}$$

where ν_L is the Landau damping rate, and the energy densities deposited in a hot-electron component and a plasma wave are given as

$$W_h=n_h(mv_{ph}^2/2), \quad W_{EPW}=(e^2/2\varepsilon_0 k^2)|\delta n|^2. \tag{3}$$

From Eqs. (2) and (3) we finally obtain the equations for hot-electron generation by the two daughter EPW's:

$$dn_{h1,2}/dt=(\nu_{L1,2}/n_0)|\delta n_{1,2}|^2-\gamma_{h1,2}n_{h1,2} \tag{4}$$

where we have introduced a sink term in which γ_h stands for the hot-electron collisional damping rate.

Assuming that the instability operates only in a well-localized region near the quarter-critical density, we can now search for the time-dependent local solutions for the slowly varying amplitudes. The neglect of convective terms in Eqs. (1) is justified provided the leading frequency in the Fourier spectrum strongly dominates the value v_g/L, where v_g is the largest among the four wave group velocities. We proceed with normalizing the above equations by introduction of the dimensionless amplitudes $a=E_0(t)/E_0(0)$, $N_{1,2,s}=\delta n_{1,2,s}(t)/n_0$, as well as the time variable $\tau=\omega_0 t$ and the frequency mismatch $\Omega=\Delta\omega/\omega_0$. Thus the final set of equations describing the temporal evolution of the process takes the form

$$\begin{aligned}
da/d\tau&=-B_0N_1N_2,\\
dN_1/d\tau&=B_1aN_2^*-C_1N_2N_s\exp(i\Omega t)-\Gamma_1N_1,\\
dN_2/d\tau&=B_2aN_1^*+C_2N_1N_s^*\exp(-i\Omega t)-\Gamma_2N_2,\\
dN_s/d\tau&=C_3N_1N_2^*\exp(-i\Omega t),\\
dh_{1,2}/d\tau&=(\alpha/\omega_p)\nu_{1,2}|N_{1,2}|^2-\Gamma_{h1,2}h_{1,2},
\end{aligned} \tag{5}$$

where the coupling coefficients are

$$\begin{aligned}
B_0&=\alpha^3\kappa_\perp(\kappa_1^2-\kappa_2^2)/2\kappa_1^2\kappa_2^2,\\
B_{1,2}&=\kappa_\perp(\kappa_1^2-\kappa_2^2)/8\alpha\kappa_{2,1}^2,\\
C_{1,2}&=\alpha^3|\vec{\kappa}_1\cdot\vec{\kappa}_2|/4\beta_e^2\kappa_{2,1}^2\kappa_s,\\
C_3&=\beta_e\sqrt{Zm/M_i}\,\kappa_s^3|\vec{\kappa}_1\cdot\vec{\kappa}_2|/4\kappa_1^2\kappa_2^2
\end{aligned}$$

and

$$\alpha=\omega_p/\omega_0, \quad \beta_e=v_e/c=\sqrt{T_e(\mathrm{keV})/511},$$

v_e designating the electron thermal velocity corresponding to the electron plasma temperature T_e. The electron-ion mass ratio is taken to be $Zm/M_i=1/3600$ in our simulations. The wave vectors of all the waves are normalized as $\kappa=ck/\omega_0$ and can easily be obtained from the geometry of the instability for the case of the most unstable modes [7]:

$$\begin{aligned}
\kappa_{1,2}&=\frac{1}{2}[(1-2\alpha)/3\beta_e^2\pm\sqrt{(1-\alpha^2)(1-2\alpha)/3\beta_e^2}],\\
\kappa_\perp&=\frac{1}{2}\sqrt{(1-2\alpha)/3\beta_e^2-(1-\alpha^2)},\\
\kappa_s&=|\vec{\kappa}_1-\vec{\kappa}_2|.
\end{aligned} \tag{6}$$

Clearly, the wave vectors as well as the scattering angles for the optimal case of maximum instability at given plasma density depend only on α and β_e. Nonoptimal instability increments would yield negligible values of density fluctuations and therefore have not been considered. The damping rates for plasma waves ($\Gamma_{1,2}$) and for hot electrons ($\Gamma_{h1,2}$) are normalized to ω_0. Note that the relations (6) impose the plasma temperature limit for the occurrence of TPD at the plasma density n_0: $T_e(\mathrm{keV})\leqslant 170.33(1-2\sqrt{n_0/n_{cr}})/(1-n_0/n_{cr})$. For example, the latter condition gives a limit around 20 keV for $n_0=0.245n_{cr}$.

III. RESULTS AND DISCUSSION

On the basis of the system of differential equations (5) we first consider the evolution of the waves involved in the process, when a very long constant intensity laser pulse propagates through a homogeneous or nearly homogeneous plasma. A typical set of physical parameters is utilized: the laser intensity parameter $a=0.03$, corresponding to an intensity of 10^{15} W cm^{-2} for the 1 μm laser, plasma density $n_0=0.246n_{cr}$, and electron temperature $T_e=0.2$ keV. The temporal behavior of the two daughter plasma wave amplitudes as well as of the ion-acoustic wave amplitude is shown in Fig. 1. The time axis is labeled in picoseconds for physical clarity. We can see in Fig. 1(a) that the maximum fluctuation amplitude N_1 of the first plasma wave, with larger wave vector, exceeds 20% at the initial stage of the process and saturates after a short time, of the order of a picosecond, which corresponds to times of the order of 10 ps when CO_2 lasers are utilized. This saturation occurs simultaneously with the ion fluctuation amplitude reaching its maximum value, somewhat below 1% for our simulation parameters. These facts stand in a very good agreement with recent experimental evidence [7]. However, the N_1 amplitude decreases slowly in time because a part of its energy experiences a flow to the other plasma wave mode N_2. Another reason for this amplitude reduction, as will be shown later, is the fact that Landau damping of this mode is mainly responsible for hot-electron generation, and the hot electrons carry away a part of the wave energy. On the other hand, Fig. 1(b) clearly shows that the second plasma wave does not experience any significant change of the initially saturated amplitude, corresponding to maximum density fluctuations of

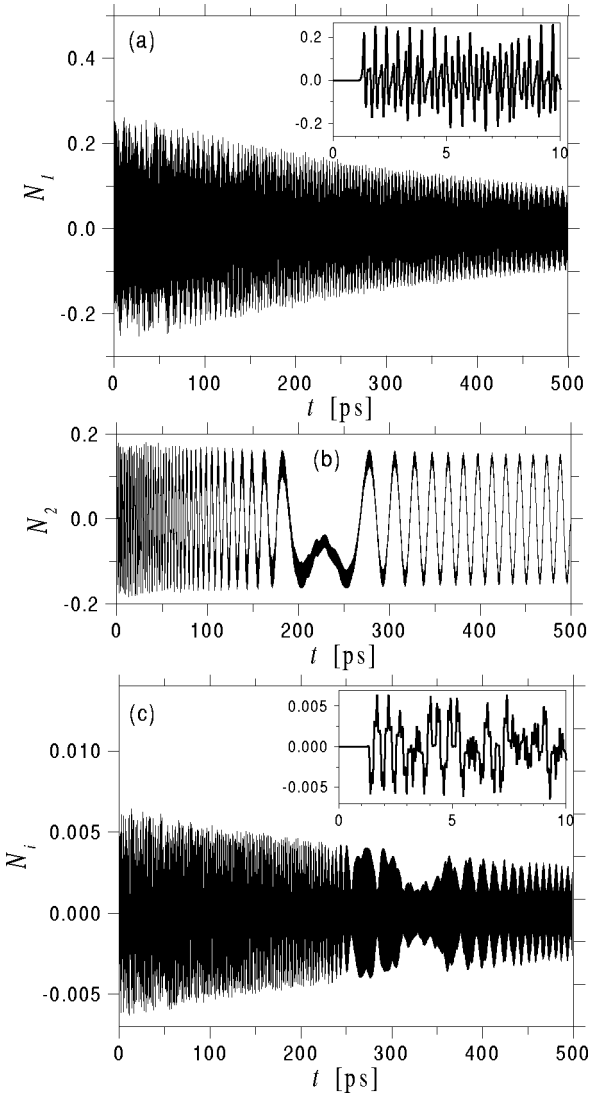

FIG. 1. Time evolution of the coupled plasma waves (a) and (b), and the ion-acoustic wave (c), for the parameters $a=0.03$, $n_0=0.246n_{cr}$, $T_e=0.2$ keV.

nearly 18% of the equilibrium plasma density.

Another interesting aspect of the plasma wave behavior is observed by deeper insight into the microscopic evolution on the picosecond scale [see the enlarged time pattern inside Fig. 1(a)]. A superficial oversight of the figure reveals at least two characteristic frequency modes, which differ by two orders of magnitude. The higher frequencies are clearly related to the ion fluctuations, as may be seen by comparison of Figs. 1(a) and 1(c), while the lower frequencies are due to inclusion of the frequency mismatch $\Delta\omega$, and are absent in the case of perfect matching. Unlike the case of the complex dynamics of N_1, the second plasma wave exhibits a relatively simple periodic behavior, with an increasing period of oscillations. The cause of this effect is a slow decrease of the laser pump amplitude, not shown here, which leads to reduction of the TPD growth rate, and consequent decrease of the slope of the N_2 amplitude variation. After a transient time of about 300 ps a recognizable quasiperiodic dynamics with two main characteristic frequencies in the amplitude evolution is established. The microdynamics of this wave mode is more regular than that of N_1. The maximum amplitude of the ion-acoustic wave reaches a value of about 0.6% at the initial stage, and is even less at further stages of the process. Nevertheless, even such relatively low values of the ion fluctuations turn out to be sufficient to procure saturation of the instability and to sustain the whole process. The latter fact has already been noticed by earlier authors [7,14], and it justifies the introduction of secondary coupling between electron and ion modes.

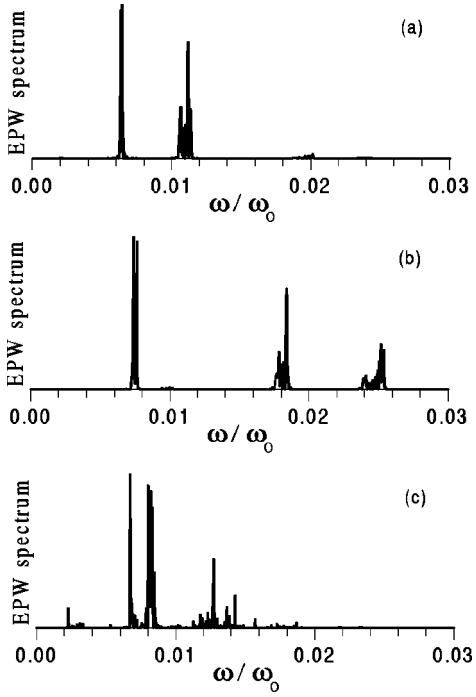

FIG. 2. Frequency spectra of the forward-propagating plasma wave slowly varying amplitude, for the parameters (a) $a=0.02$, $T_e=0.2$ keV; (b) $a=0.03$, $T_e=0.2$ keV; (c) $a=0.02$, $T_e=0.35$ keV. For all the cases $n_0=0.246n_{cr}$.

As the forward propagating plasma wave exhibits a complex physical behavior, our attention has been focused on the frequency spectra of this mode for various laser and plasma parameters. First, we produce spectra corresponding to slowly varying wave envelopes, from data corresponding to those given in Fig. 1(a). A deeper inspection of the amplitude oscillation patterns reveals that typical oscillation periods are of the order of a fraction of a picosecond, whereas the laser period for the present wavelength is only about 3 fs. Thus, the fact that the dominant oscillation frequency of the EPW amplitude is of the order of $10^{-2}\omega_0$ justifies our assumption that the amplitude changes slowly in time. It is also possible now to evaluate the adequacy of our neglect of the convective terms in Eqs. (1); namely, this dominant frequency is obviously much greater than the ratio of the maximum group velocity in the system and the characteristic plasma scale length. For example, for millimeter-scale-length plasmas, the dominant oscillation frequency is greater than this ratio by two orders of magnitude.

For comparison and estimation of the effect of the parameter variation, we give in Fig. 2(a) the spectra for the param-

eters $a=0.02$, $n_0=0.246n_{cr}$, and $T_e=0.2$ keV. Then we change the laser intensity to $a=0.03$ [Fig. 2(b)] and the plasma temperature to $T_e=0.35$ keV in Fig. 2(c). Two characteristic spectral lines are clearly distinguishable, as expected on the basis of the previous discussion. The main spectral line in Fig. 2(a) lies at a frequency just above $\sim 0.006\omega_0$, while the second one is not clearly defined in frequency and seems to be composed of two very close components with frequencies about $0.011\omega_0$. Figure 2(b) clearly reveals blueshifts in the spectra with increasing laser intensity. However, while the lower-frequency line experiences just a slight, hardly observable shift, the corresponding blueshift of the second spectral line proves to be much larger and proportional to the pump strength a. We can verify by inspection that the third line appearing in Fig. 2(b) is just a combination frequency, generated by beating of the first two lines. In this way we conclude that we still do not have three incommensurate frequencies in the system, which would be an indication of the route to chaos. In other words, the dynamics retains its quasiperiodic character for realistic physical parameters. So the general conclusion is that the richness and complexity of the scattering process physics increase rapidly with laser intensity, followed by spectral line broadening and more and more pronounced modulation. The maximum saturation amplitudes of both plasma waves and the ion-acoustic wave have the same dependence. All these effects are easily understandable having in mind that the efficiency of the primary nonlinear coupling process increases with increasing pump intensity, owing to the fact that the growth rate of TPD is proportional to the electron quiver velocity, leading to more rapid variations of the plasma wave amplitude.

Further analysis of the data presented in Fig. 2 reveals that the complexity of the frequency spectra, as well as the spectral line width and line modulation, increase with the temperature of the bulk plasma. With further increase of the temperature, the spectrum would become broader and essentially continuous, with no pronounced frequencies. All this illustrates the pronounced role of thermal electron motion in TPD physics, which makes theoretical predictions unreliable for the case of higher plasma temperatures.

Next we consider the frequency spectra generated on the basis of the complete wave function of the plasma wave, obtained by multiplying the slowly varying amplitudes by the corresponding phase factors $\exp(i\omega_{1,2}t)$, where $\omega_{1,2}$ are the exact frequencies of the daughter EPW's. These are more convenient for comparison with the experimentally obtained ones than the spectra shown in Fig. 2. Two such spectra displayed in Fig. 3 correspond to the parameters of the slowly varying amplitude spectra shown in Figs. 2(a) and 2(b). The two main peaks appearing in the figures are obviously generated from the highest peaks in Figs. 2(a) and 2(b), in convolution with the phase function $\exp(i\omega t)$, and they are supposed to be each other's mirror images. However, the generated spectra are clearly asymmetric, which comes from the complex quasiperiodic dynamics of the plasma waves involved in the coupling process. It is an extremely difficult task to follow the plasma wave dynamics directly in the laboratory, although this was achieved in

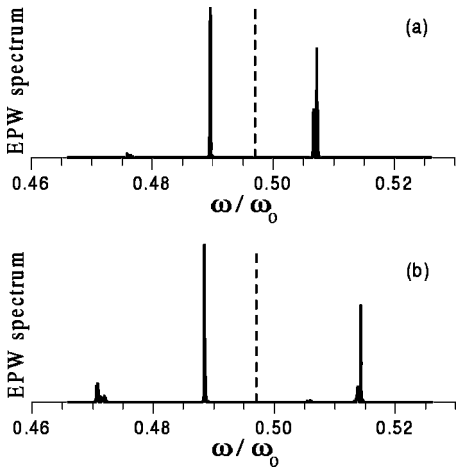

FIG. 3. Frequency spectra of the forward-propagating plasma wave fast wave function, for the parameters of Figs. 2(a) and 2(b). The dashed line designates the EPW fiducial for $n_0=0.246n_{cr}$.

laser-plasma experiments by Baldis and Walsh and some other researchers, by using the Thomson scattering method [11,13,16]. As for the plasma waves from TPD, it has been much more usual to draw conclusions indirectly, by observing the $(3/2)\omega$ radiation or $\omega/2$ radiation from the plasma [14,17,18]. Odd-integer half harmonics are supposed to be generated by nonlinear coupling between the incident laser light of frequency ω and the plasma waves induced by TPD or Raman scattering in the quarter-critical region, whose frequency is about $\omega/2$. We believe that there exists a close correspondence between the plasma wave spectra and experimentally observed $(3/2)\omega$ spectra. The main features of the latter spectra are their asymmetry and a strong dependence of the separation between red- and blueshifted peaks on the laser and plasma parameters. Thus, in the experiment of Figueroa *et al.* [19] this separation appears proportional to the square root of laser intensity I, i.e., proportional to the earlier introduced parameter a. This is just what we observe in Figs. 3(a) and 3(b), in which separations between peaks stand in the ratio 2:3, corresponding to the laser parameters used ($a=0.02$ and 0.03, respectively). Another important fact is the separation dependence on the plasma temperature T_e. Researchers usually assume that this separation is proportional to plasma temperature, which is derived from the standard theory of $(3/2)\omega$ radiation generation [2,14,20]. However, according to our model the separation is expected to scale as $T_e^{1/2}$, because the leading frequency in the spectrum (Fig. 2) is supposed to be closely related to the ion-acoustic frequency, which is proportional to the square root of the electron temperature. Thus, we offer an alternative explanation of the origin of the asymmetry and other peculiarities of the $(3/2)\omega$ spectra. In this scheme, of the two TPD-induced plasma waves, only the one more unstable to Langmuir decay (the one with larger **k**) contributes to the eventual $(3/2)\omega$ or $\omega/2$ spectra.

We now turn to analysis of the hot-electron generation process, described by the last equation of the system (5). As expected, our simulations indicate that the number of hot electrons generated during the process, as well as their gen-

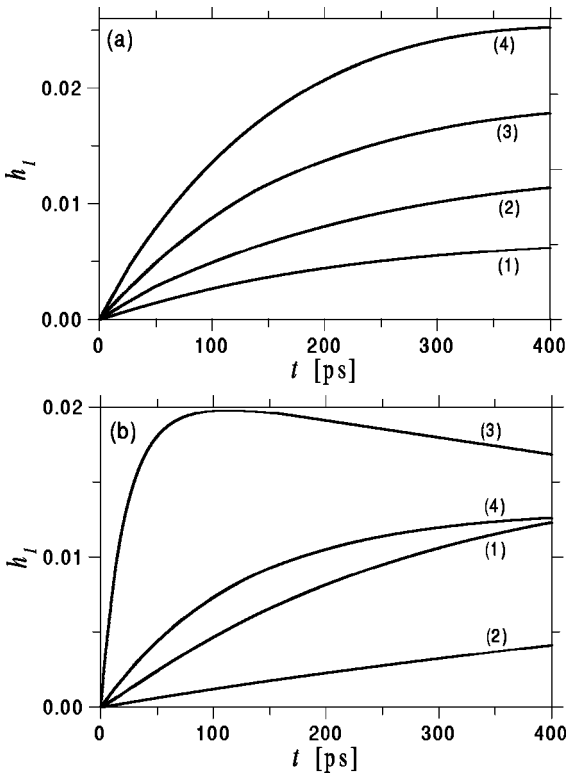

FIG. 4. The hot-electron density versus time for the following parameter sets: (a) $T_e=0.2$ keV, $n_0=0.246n_{cr}$, and $a=0.02$, 0.03, 0.04, and 0.05 (curves 1–4); (b) $T_e=0.35$ keV, $n_0=0.245n_{cr}$ (1), $T_e=0.4$ keV, $n_0=0.245n_{cr}$ (2), $T_e=0.4$ keV, $n_0=0.244n_{cr}$ (3), and $T_e=0.5$ keV, $n_0=0.244n_{cr}$ (4), all for $a=0.04$.

eration rate, is strongly affected by both laser and plasma parameters.

In Fig. 4(a), the temporal evolution of the normalized hot-electron density is displayed for the case of the plasma density $n_0=0.246n_{cr}$ and electron temperature $T_e=0.2$ keV. The laser intensity a takes the values 0.02, 0.03, 0.04, and 0.05 (curves 1–4, respectively). Clearly, both the number and the generation rate of hot electrons increase with laser light intensity. The explanation is straightforward: TPD growth rate increases with increase of the pump intensity, thus leading to faster growth of the EPW amplitudes. Larger amplitude EPW's then accelerate larger numbers of resonant electrons to their phase velocities. Initially, the hot-electron number growth is linear; however, when the EPW-induced electron density fluctuation exceeds 10%, a sink mechanism, based on hot-bulk electron collisions, begins to operate, causing efficient hot-electron generation saturation. For the present parameters, which are typical for a class of TPD experiments, the number of generated hot electrons saturates at values between fractions of a percent and a few percent in respect to bulk electrons. This result is quite in accordance with the present, not very rich, experimental evidence. Experimentally, hot electrons are rarely counted directly [19,21]. More frequently an indirect method is used, based on detection of x rays launched by the decelerated electrons [3,4,22]. Related calculations show that the hot-electron fraction ranges between 0.1% and 10%, which justifies the results of the presented model.

In Fig. 4(b), the temporal evolution of hot-electron density for a range of plasma densities and temperatures is shown, corresponding to the same laser intensity $a=0.04$, revealing the hot-electron generation dependence on these parameters. We see that even during the laser pulse the number of hot electrons generated may reach its maximum and then slowly decrease, owing to the fact that the collisional sink term exceeds the generation rate. It is also observed that the increase in temperature as well as the approach to the quarter-critical density reduce the hot-electron generation; namely, in both cases more bulk electrons are shifted toward greater energies, thus reducing the number of resonant electrons among which hot electrons are recruited. In other words, the hotter or denser the plasma, the smaller the wave vector. This leads to a lower value of the Landau damping rate, resulting in a decreased number of generated hot electrons.

IV. SUMMARY

An attempt was made to develop a simple, transparent, nonlinear model of TPD in a long-scale-length plasma, including a number of the most prominent plasma nonlinearities. The model is made for the case of maximum TPD growth rate, under the assumption that all the amplitudes of the waves participating in the process vary slowly in time and that all the convective terms may be neglected, because the dominating frequency in the slowly varying amplitude spectrum greatly exceeds the ratio of the maximum group velocity in the system and the characteristic plasma scale length.

Our simulations confirm the assumption that coupling of the EPW's generated in the primary process of TPD with the ion-acoustic waves provides an efficient saturation mechanism for the instability, despite relatively small amplitudes of these ion fluctuations. Due to the nonresonant nature of the secondary coupling between the EPWs and the ion-acoustic wave, a frequency mismatch is introduced, which proves to contribute to the rich dynamics of the process. It leads to the frequency lines shifting and broadening, as well as an increase of their complexity, and the appearance of new spectral lines corresponding to lower-frequency oscillations. The increase of the pump strength causes increased complexity of the corresponding spectra, as well as spectral line broadening and more pronounced modulation, due to the increase of the primary nonlinear coupling efficiency. The same effect is achieved by an increase of the plasma electron temperature.

An attempt has been made to explain the experimentally observed asymmetry and other peculiarities of the spectrum of $(3/2)\omega$ radiation, which is tightly related to the TPD process. The separation dependence of the spectral line splitting in the frequency spectra is found to depend on the plasma temperature T_e and the separation is expected to scale as $T_e^{1/2}$.

The hot-electron density and generation rate are found to be strongly dependent on the plasma and laser parameters,

due to the sensitivity of the Landau damping rate to these parameters. As expected, the number and generation rates of the hot electrons increase with laser light intensity, for constant a and T_e, owing to the fact that the TPD growth rate increases with the pump intensity. At the same time they decrease with increasing bulk electron temperature and density, for constant a, due to the decrease of the number of resonant electrons from which the hot electrons are recruited.

ACKNOWLEDGMENT

This work was supported in part by the Ministry of Sciences of Serbia, through Project No. 1964.

[1] W. L. Kruer, *The Physics of Laser Plasma Interactions* (Addison-Wesley, Redwood City, CA, 1988).
[2] H. A. Baldis, E. M. Campbell, and W. L. Kruer, in *Handbook of Plasma Physics: Physics of Laser Plasma*, edited by A. M. Rubenchik and S. Witkowski (Elsevier Science Publishers, Amsterdam, 1991), p. 361.
[3] B. Yaakobi, C. Stoecki, T. Boehly, D. D. Meyerhofer, and W. Seka, Phys. Plasmas **7**, 3714 (2000).
[4] F. C. Young, M. J. Herbst, C. K. Manka, S. P. Obenschain, and J. H. Gardner, Phys. Rev. Lett. **54**, 2509 (1985).
[5] A. B. Langdon, B. F. Lasinski, and W. L. Kruer, Phys. Rev. Lett. **43**, 133 (1979).
[6] C. S. Liu and M. N. Rosenbluth, Phys. Fluids **19**, 967 (1976).
[7] J. Meyer and Y. Zhu, Phys. Rev. Lett. **71**, 2915 (1993).
[8] S. J. Karttunen, Phys. Rev. A **23**, 2006 (1981).
[9] R. W. Short, W. Seka, K. Tanaka, and E. A. Williams, Phys. Rev. Lett. **52**, 1496 (1984).
[10] B. B. Afeyan and E. A. Williams, Phys. Plasmas **4**, 3827 (1997).
[11] H. A. Baldis and C. J. Walsh, Phys. Fluids **26**, 1364 (1983).
[12] D. F. DuBois, D. A. Russell, and H. A. Rose, Phys. Rev. Lett. **74**, 3983 (1995).
[13] C. Labaune, H. A. Baldis, B. S. Bauer, V. T. Tikhonchuk, and G. Laval, Phys. Plasmas **5**, 234 (1998).
[14] J. Meyer, Phys. Fluids B **4**, 2934 (1992).
[15] A. A. Offenberger, R. Fedosejevs, W. Tighe, and W. Rozmus, Phys. Rev. Lett. **49**, 371 (1982).
[16] K. L. Baker *et al.*, Phys. Plasmas **4**, 3012 (1997).
[17] R. E. Turner, D. W. Philion, B. F. Lasinski, and E. M. Campbell, Phys. Fluids **27**, 511 (1984).
[18] T. A. Peyser, C. K. Manka, S. P. Obenschain, and K. J. Kearney, Phys. Fluids B **3**, 1479 (1991).
[19] H. Figueroa, C. Joshi, H. Azechi, N. A. Ebrahim, and K. Estabrook, Phys. Fluids **27**, 1887 (1984).
[20] D. M. Villeneuve, H. A. Baldis, and C. J. Walsh, Phys. Fluids **28**, 1454 (1985).
[21] N. A. Ebrahim, H. A. Baldis, C. Joshi, and R. Benesch, Phys. Rev. Lett. **45**, 1179 (1980).
[22] D. W. Phillion, E. M. Campbell, K. G. Estabrook, G. E. Phillips, and F. Ze, Phys. Rev. Lett. **49**, 1405 (1982).